Published in IET Circuits, Devices & Systems
Received on 3rd May 2010
Revised on 14th July 2010
doi: 10.1049/iet-cds.2010.0141

ISSN 1751-858X

Field programmable analogue array implementation of fractional step filters

T.J. Freeborn[1] *B. Maundy*[1] *A.S. Elwakil*[2]

[1]*Department of Electrical and Computer Engineering, University of Calgary, Calgary, Alberta, Canada*
[2]*Department of Electrical and Computer Engineering, University of Sharjah, P.O. Box 27272, Sharjah, United Arab Emirates*
E-mail: bmaundy@ucalgary.ca

Abstract: In this study, the authors propose the use of field programmable analogue array hardware to implement an approximated fractional step transfer function of order $(n+\alpha)$ where n is an integer and $0 < \alpha < 1$. The authors show how these filters can be designed using an integer order transfer function approximation of the fractional order Laplacian operator s^{α}. First and fourth-order low- and high-pass filters with fractional steps from 0.1 to 0.9, that is of order 1.1–1.9 and 4.1–4.9, respectively, are given as examples. MATLAB simulations and experimental results of the filters verify the implementation and operation of the fractional step filters.

1 Introduction

Traditionally the Laplacian operator, s, is raised to an integer order, that is, s, s^2, …, s^n, when used in the design of analogue circuits. However, it is also mathematically valid to raise it to a non-integer order, s^{α}, where $\alpha \epsilon \Re$ representing the differintegrator [1] also referred to in this work as the fractional Laplacian operator. A fractional derivative of order α is given by the Grünwald–Letnikov approximation [2] as

$$D^{\alpha}f(t) \triangleq \lim_{\Delta T \to 0} \frac{(\Delta T)^{-\alpha}}{\Gamma(-\alpha)} \sum_{j=0}^{\infty} \frac{\Gamma(j-\alpha)}{\Gamma(j+1)} f(t-j\Delta T) \quad (1)$$

where ΔT is the integration step and $\Gamma(\cdot)$ is the gamma function. Applying the Laplace transform to (1) yields

$$L\{D^{\alpha}f(t)\} = s^{\alpha}F(s) \quad (2)$$

Although there are no physical analogies to these derivatives, like slope or area under the curve, the concepts of fractional calculus and fractional-order systems have slowly been migrating into engineering showing many useful applications in diverse fields. These include materials theory, diffusion theory, bioengineering, circuit theory and design [1], control theory [3, 4], electromagnetics [5] and robotics [6, 7]. The import of these concepts into circuit theory is relatively new, and has shown applications in transmission media [2], power electronics [8], integrator [9, 10] and differentiator circuits [11], oscillators [12], multivibrator circuits [13] and filter theory [14–17] with potentially many other applications.

The fractional Laplacian operator is especially useful in the design of filters with fractional step characteristics in the stopband, as the design of transfer functions can be done algebraically rather than through solving the difficult time domain representations of the fractional derivatives. The stopband attenuation of integer order filters has been limited to increments based on the order, n, but using the fractional Laplacian operator attenuations between these integer steps can be achieved creating a fractional step filter of order $(n+\alpha)$, where α is the fractional step between integer orders n and $n+1$ and is therefore limited to $0 < \alpha < 1$. Previous work on fractional step filters [14, 15] has shown these filters to be realisable with precise control of the stopband characteristics. However, using the transfer function in [14] of order $(1+\alpha)$ yields an undesired peaking in the passband that increases with increasing α. Using the fractional transfer functions proposed in [18] a fractional step through the stopband region is achieved while eliminating the undesired passband peaking and maintaining a flat passband response through appropriate selection of the constants $k_{2,3}$ in [18]. The elimination of

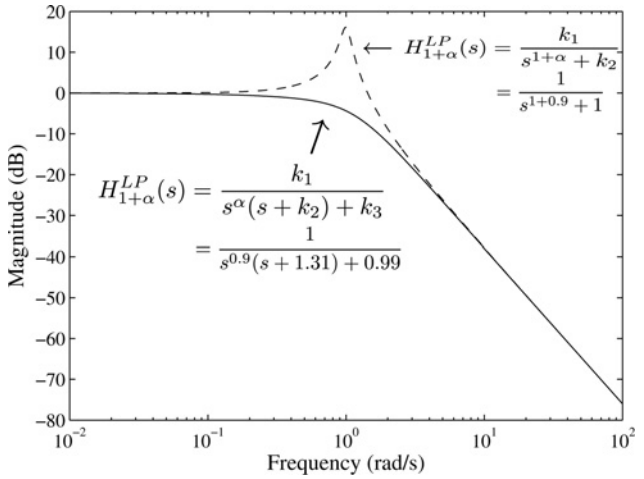

Figure 1 *Comparison of magnitude responses of FLPFs of order $(1+\alpha) = 1.9$ from [14, 18]*

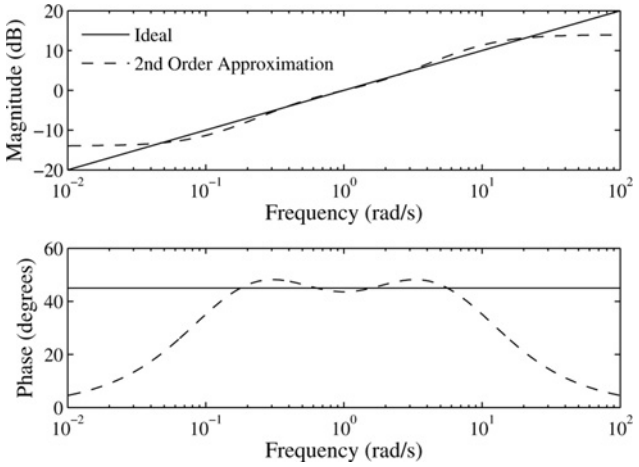

Figure 2 *Magnitude and phase of $s^{0.5}$ using second-order approximation (dashed) compared to ideal case (solid)*

the passband peaking in the magnitude response using the proposed fractional low-pass transfer function in [18] of order $(1+\alpha)$ compared to that previously proposed in [14] is shown in Fig. 1 for the case when $\alpha = 0.9$ with constants $k_2 = 1.31$ and $k_3 = 0.99$.

In this paper, we explore the feasibility of the new approximation to the fractional step filter design using a field programmable analogue array (FPAA) as a means of implementation and test. We use a second-order approximation for the fractional Laplacian operator to realise both fractional low-pass filter (FLPF) and fractional high-pass filter (FHPF) of orders $1.1 \rightarrow 1.9$ and $4.1 \rightarrow 4.9$. MATLAB simulations are verified experimentally using the FPAA. The precise attenuation control offered by these filters is highlighted using approximated fractional high-pass filters of order $4.1 \rightarrow 4.9$ against fourth- and fifth-order standard highpass Butterworth filters [19–21].

2 Approximation of the fractional Laplacian operator

The use of the fractional Laplacian operator, s^{α}, has theoretically been shown to produce filters with a fractional step through the stopband [14, 15, 17]. However, there are no commercial fractance devices available for the physical realisation of these filters. Although most capacitors do exhibit fractional behaviour [22, 23] and should be modelled with impedance $Z_C = 1/s^{\alpha}C$, the value of α is very near to 1 preventing their use in implementing fractional filters with complete control of the stopband attenuations. Therefore until commercial fractance devices become available to physically realise circuits that make use of the advantages of s^{α}, integer order approximations have to be used. There are many methods used to create an approximation of s^{α} that include continued fraction expansions (CFEs) as well as rational approximation methods [3]. These methods present a large array of approximations with varying order and accuracy, with the accuracy and approximated frequency band increasing as the order of the approximation increases. Using the CFE method of [24] we obtain the following approximation for the general Laplacian operator to second order

$$s^{\alpha} \approx \frac{(\alpha^2+3\alpha+2)s^2+(8-2\alpha^2)s+(\alpha^2-3\alpha+2)}{(\alpha^2-3\alpha+2)s^2+(8-2\alpha^2)s+(\alpha^2+3\alpha+2)} \quad (3)$$

Note that when $\alpha = 0.5$, (3) reverts back to the approximation of $s^{0.5}$ in [24]. Fig. 2 shows an example of the magnitude and phase of the approximation of the fractional Laplacian operator for the case when $\alpha = 0.5$ compared to the ideal case. It can be observed that for $\omega \in [0.032, 31.53]$ the magnitude error does not exceed 1.375 dB while for $\omega \in [0.142, 7.00]$ the phase error does not exceed 3.2°. Using a second-order approximation for the Laplacian operator results in an $(n+2)$ integer order filter to approximate the $(n+\alpha)$ fractional step filter, which is less expensive to implement in hardware over approximations of higher order [3, 25].

3 Fractional step filters

Using the approximation of the fractional Laplacian operator in (3), a fractional step low-pass transfer function of the form

$$H_{1+\alpha}^{\mathrm{LP}}(s) = \frac{k_1}{s^{\alpha}(s+k_2)+k_3} \quad (4)$$

changes to

$$H_{1+\alpha}^{\mathrm{LP}}(s) \approx \frac{k_1}{a_0}\frac{(a_2s^2+a_1s+a_0)}{s^3+c_0s^2+c_1s+c_2} \quad (5)$$

where $a_0 = \alpha^2+3\alpha+2$, $a_1 = 8-2\alpha^2$, $a_2 = \alpha^2-3\alpha+2$, $c_0 = (a_1+a_0k_2+a_2k_3)/a_0$, $c_1 = (a_1(k_2+k_3)+a_2)/a_0$ and

$c_2 = (a_0k_3 + a_2k_2)/a_0$. Through careful selection of $k_{2,3}$ the passband region can be shaped while maintaining the desired fractional step through the stopband. To create a flat passband the constants $k_{2,3}$ when $k_1 = 1$ that yield the minimum cumulative passband error when compared to the Butterworth response (The Butterworth response was chosen because it offers a maximally flat passband response. However, the use of Chebychev or Bessel filters is also possible.) over a select frequency range, were calculated numerically. These cumulative magnitude errors, $|E_C(j\omega)|$, can be calculated as

$$|E_C(j\omega)| = \sum_{i=1}^{N} | \, |B_1(j\omega_i)| - |H_{1+\alpha}^{LP}(j\omega_i)| \, | \qquad (6)$$

where $|B_1(j\omega_i)|$ is the magnitude response at frequency ω_i of the first order low-pass Butterworth filter, $|H_{1+\alpha}^{LP}(j\omega_i)|$ is the magnitude response of the FLPF of order $(1+\alpha)$ at frequency ω_i, and N is the number of samples. For our analysis 200 samples were taken over the frequency range $\omega \epsilon [0.01, 1]$. For each value of α between 0.01 and 0.99 in steps of 0.01, the cumulative error was calculated for all combinations of $0 < k_2 < 2$ and $0 < k_3 < 1$ in steps of 0.001. From all the cumulative errors collected for each α value, the combination that resulted in the minimum error was selected. These values that yield the minimum cumulative passband error when using the approximation as well as the interpolated functions to match the collected data are shown in Fig. 3 as solid and dashed lines, respectively. The interpolated quadratic and linear functions from the collected raw data for k_2 and k_3, respectively, are found as

$$k_2 = 1.0683\alpha^2 + 0.161\alpha + 0.3324 \qquad (7)$$

$$k_3 = 0.29372\alpha + 0.71216 \qquad (8)$$

with a norm of residuals (The norm of residuals is calculated from the fit residuals, defined as the difference between the ordinate data point and the resulting fit for each abscissa data point; with a lower norm value indicating a better fit than a larger value.), R, of 0.15239 and 0.034421 for the interpolated functions of k_2 and k_3, respectively.

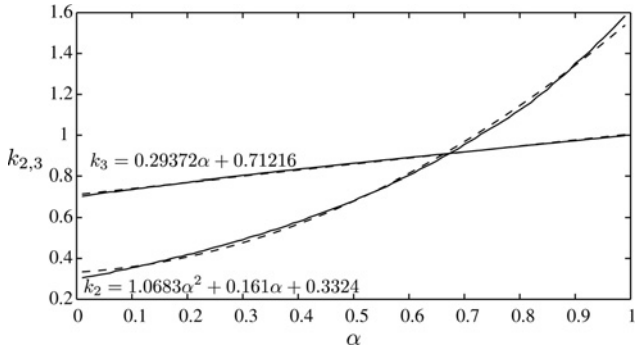

Figure 3 *Plot of k_2 and k_3 against α that yields minimum passband error in (5) and the interpolated functions as solid and dashed lines, respectively*

4 FPAA implementation

Anadigm FPAAs are 'analogue signal processors' consisting of fully configurable analogue modules (CAMs) surrounded by programmable interconnect and analogue input/output cells [26]. The signal processing occurs in the CAMs using fully differential switched capacitor circuitry, which provide specialised behaviours such as filtering, gain, sample and hold, summing, rectification and more. This provides a very flexible architecture that can be easily reconfigured using the AnadigmDesigner tools. These tools are a graphical design environment to build circuits using the design CAMs. In this design environment CAMs can be dropped in, wired together and configured for the desired design requirements. From the graphical implementation of a circuit, the AnadigmDesigner tools generate the configuration data file to program the FPAA.

Two CAMs that are particularly useful in the implementation of approximated fractional step filters are the bilinear and biquadratic filter CAMs. The cascaded connection of these CAMs in the AnadigmDesigner environment is shown in Fig. 4. These CAMs realise bilinear and biquadratic transfer functions given the pole and zero frequencies and quality factors making them ideal for the realisation of filters that have been decomposed into biquadratic and bilinear sections. Previous discrete component realisations of approximated FLPFs [18] required the use of the design equations from [27] to determine the component values to realise the biquadratic transfer function using the STAR-SAB topology [28]. Therefore using the biquadratic and bilinear filter CAMs from the AnadigmDesigner tools greatly reduces both the number of calculations and time required to physically implement approximated fractional step filters.

4.1 Fractional low-pass filter

To realise the transfer function of (5) we decompose it into first- and second-order transfer functions that can be realised using bilinear and biquadratic filter CAMs, respectively. For our realisation, the two transfer functions generated were

$$H(s) = H_1(s)H_2(s) = \frac{1}{s + d_0} \frac{e_0s^2 + e_1s + e_2}{s^2 + d_1s + d_2} \qquad (9)$$

where $H_1(s)$ and $H_2(s)$ represent first- and second-order transfer functions, respectively. Coefficients $d_{0,1,2}$ and $e_{0,1,2}$ can be determined through the numerical solution of the system of equations obtained from equating the terms of

doi: 10.1049/iet-cds.2010.0141

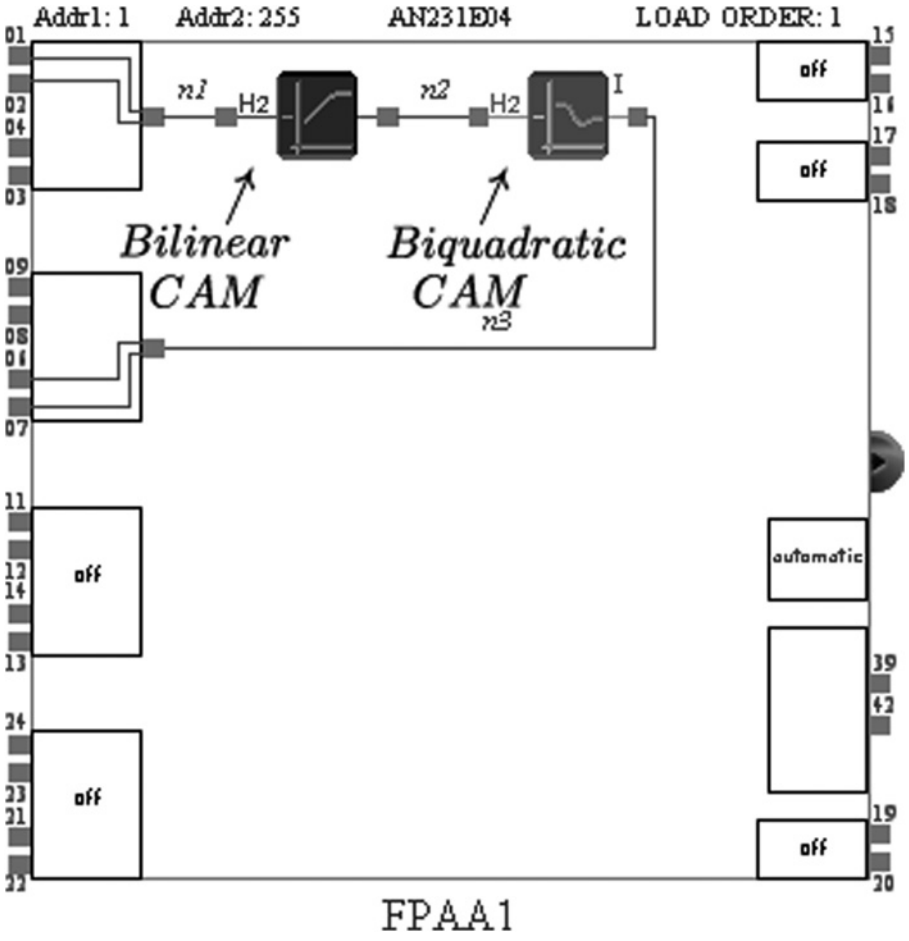

Figure 4 *Cascaded connection of the bilinear and biquadratic filter CAMs in the AnadigmDesigner environment*

(5) and (9), resulting in the following system of equations

$$\begin{aligned} d_0 + d_1 &= \frac{a_1 + a_0k_2 + a_2k_3}{a_0} \\ d_0d_1 + d_2 &= \frac{a_1(k_2 + k_3) + a_2}{a_0} \\ d_0d_2 &= \frac{a_0k_3 + a_2k_2}{a_0} \\ e_0 &= k_1\frac{a_2}{a_0} \\ e_1 &= k_1\frac{a_1}{a_0} \\ e_2 &= k_1 \end{aligned} \tag{10}$$

The transfer function of (9) must also be arranged to match the CAMs, taking the form

$$\begin{aligned} H(s) &= T_1(s)T_2(s) \\ T_1(s) &= \frac{2\pi f_1G_1}{s + 2\pi f_1} \\ T_2(s) &= -\frac{s^2 + (2\pi f_{2_z})/(Q_{2_z})s + 4\pi^2f_{2_z}^2}{s^2 + (2\pi f_{2_p})/(Q_{2_p})s + 4\pi^2f_{2_p}^2} \end{aligned} \tag{11}$$

where $T_1(s)$ and $T_2(s)$ are the transfer functions of the bilinear and biquadratic filter CAMs, respectively. Here G_1 is the gain of $T_1(s)$, f_1 the pole frequency of $T_1(s)$, $f_{2_{p,z}}$ the pole and zero frequencies of $T_2(s)$ and $Q_{2_{p,z}}$ the pole and zero quality factors of $T_2(s)$. Before equating the biquadratic and bilinear transfer functions of (9)–(11) the frequency transformation $s = s/\omega_o = s/2\pi f_0$ must be applied to (9), where f_0 is the denormalised frequency. The design equations to implement the approximated FLPF of order $(1 + \alpha)$ can therefore be summarised as

$$\begin{aligned} f_1 &= d_0f_0 \\ f_{2_z} &= f_0\sqrt{\frac{e_2}{e_0}} \\ Q_{2_z} &= \frac{\sqrt{e_0e_2}}{e_1} \\ f_{2_p} &= f_0\sqrt{d_2} \\ Q_{2_p} &= \frac{\sqrt{d_2}}{d_1} \\ G_1 &= \frac{e_0}{d_0} \end{aligned} \tag{12}$$

As an example the realised values of pole and zero frequencies and quality factors for both the bilinear and biquadratic CAMs, for approximated FLPFs of orders $(1+\alpha)=1.1$, 1.5 and 1.9, when $f_0=1$ kHz, are given in Table 1*a*. In Table 1*b* the values of $d_{0,1,2}$ and $e_{0,1,2}$ computed from (10) that lead to Table 1*a* for the same values of α are shown. Note the values of $k_{2,3}$ shown yield the minimum passband error with the second-order approximation of the fractional Laplacian operator when $k_1=1$. It should be mentioned that the realised values given in Table 1*a* vary from the theoretical because of the limitations on the values that can be implemented by the FPAA. The biquadratic and bilinear filter CAMs cannot realise all possible values because of hardware limits as a result of the design parameters being interrelated to other parameters as well as the sample clock frequency. The corner frequencies of both poles and zeroes are linearly related to the sample clock frequency, F_c, with the absolute upper and lower values limited to $F_c/10$ and $F_c/500$, respectively. Also, the corner frequencies, quality factors and gains are all interrelated based on the capacitors of the internal switched capacitor circuits of the FPAA. Since there are a finite number of capacitor values implemented on silicon, the AnadigmDesigner tools select the capacitor values with the best ratios to satisfy the design parameters entered. However, these best ratios do not always meet the exact parameters which results in the variation between the theoretical and realised values.

4.1.1 Higher-order FLPF design (n ≥ 2): From the stability analysis in [18] the transfer function of (4) is always unstable for $(n+\alpha)\geq 2$ when $n\geq 2$. Therefore this transfer function is not able to realise stable higher-order fractional step filters. To overcome this, it was suggested in [18] to employ $H^{\mathrm{LP}}_{1+\alpha}(s)$, which is always stable when $0<\alpha<1$, divided by higher-order normalised Butterworth polynomials [20]. This creates a stable higher-order fractional step filter of order $(n+\alpha)$ which can be written as

$$H^{\mathrm{LP}}_{n+\alpha}(s)=\frac{H^{\mathrm{LP}}_{1+\alpha}(s)}{B_{n-1}(s)},\quad n\geq 2 \tag{13}$$

where $B_n(s)$ is a standard Butterworth polynomial of order n. Using this method higher-order filters with a fractional step

Table 1 *a* Theoretical and realised biquad and bilinear CAM values for physical implementation of approximated $(1+\alpha)$ order FLPFs and *b* $d_{0,1,2}$ and $e_{0,1,2}$ values for decomposed first- and second-order transfer functions to realise an approximated FLPF of orders 1.1, 1.5 and 1.9

a						
Design value	Order $(1+\alpha)$					
	1.1		1.5		1.9	
	Theoretical	Realised	Theoretical	Realised	Theoretical	Realised
f_1, kHz	0.305	0.309	0.455	0.456	0.697	0.699
f_{2_p}, kHz	1.81	1.81	1.48	1.47	1.20	1.21
f_{2_z} kHz	1.16	1.17	2.24	2.23	7.08	7.15
Q_{2_p}	0.447	0.445	0.618	0.619	0.653	0.637
Q_{2_z}	0.249	0.249	0.224	0.225	0.122	0.122
G_1	2.43	2.40	0.439	0.429	0.0287	0.0287
b						
Value	$(1+\alpha)^{k_2}_{k_3}$					
	$(1+0.1)^{0.35}_{0.74}$	$(1+0.5)^{0.69}_{0.86}$	$(1+0.9)^{1.36}_{0.97}$			
d_0	0.3056	0.4511	0.6920			
d_1	4.0467	2.4109	1.8452			
d_2	3.2689	2.2125	1.4409			
e_0	0.7403	0.2000	0.0120			
e_1	3.4545	2.0000	1.1579			
e_2	1.0000	1.0000	1.0000			

$k_{2,3}$ shown are for minimum passband error

doi: 10.1049/iet-cds.2010.0141

through the stopband while maintaining the flat passband response can be implemented. Realising these on the FPAA requires cascading further combinations of bilinear and biquadratic filter CAMs in the AnadigmDesigner environment with those designed to implement (5). With the added CAMs designed to implement a standard low-pass Butterworth filter of order $(n-1)$ frequency shifted to f_0 to realise the $(n+\alpha)$ FLPF.

4.2 Fractional high-pass filter

To obtain a high-pass filter from its low-pass counterpart is straightforward and implies use of the LP-to-HP transformation [21]. That is, replacing s with $1/s$ in the LP transfer function, which when applied to (5) results in a high-pass filter with a fractional step through the stopband region. These FHPF can also be physically realised using the FPAA using the same pole and zero frequency and quality factor design equations of (12) and bilinear and biquadratic filter CAMs configured in the high-pass configuration. However, while the same design equations can be utilised, the values of $d_{0,1,2}$ and $e_{0,1,2}$ are different than the low-pass values and must be calculated from the following system of equations

$$\begin{aligned} d_0 d_2 &= \frac{a_0}{a_0 k_3 + a_2 k_2} \\ d_0 d_1 + d_2 &= \frac{a_0 k_2 + a_1 + a_2 k_3}{a_0 k_3 + a_2 k_2} \\ d_0 + d_1 &= \frac{a_1(k_2 + k_3) + a_2}{a_0 k_3 + a_2 k_2} \\ e_0 &= k_1 \\ e_1 &= k_1 \frac{a_1}{a_0} \\ e_2 &= k_1 \frac{a_2}{a_0} \end{aligned} \tag{14}$$

The realised values for both the bilinear and biquadratic CAMs, for approximated FHPFs of orders $(1+\alpha) = 1.1$, 1.5 and 1.9, when $f_0 = 10$ kHz are given in Table 2*a*. Correspondingly, using (14) the values of $d_{0,1,2}$ and $e_{0,1,2}$ for the same order to the values of $k_{2,3}$ that yield minimum passband error are presented in Table 2*b*. Similar to how stable higher-order FLPFs are obtained, higher-order

Table 2 *a* Theoretical and realised bilinear and biquad CAM values for physical implementation of approximated $(1+\alpha)$ order FHPFs and *b* coefficients $d_{0,1,2}$ and $e_{0,1,2}$ values for decomposed first- and second-order transfer functions to realise an approximated FHPF of orders 1.1, 1.5 and 1.9

a						
Design value	Order $(1+\alpha)$					
	1.1		1.5		1.9	
	Theoretical	Realised	Theoretical	Realised	Theoretical	Realised
f_1, kHz	34.1	32.8	21.99	21.9	14.4	14.4
f_{2_p}, kHz	5.52	5.22	6.75	6.76	8.35	8.35
f_{2_z}, kHz	8.60	8.66	4.47	4.27	1.41	1.42
Q_{2_p}	0.447	0.448	0.618	0.632	0.654	0.657
Q_{2_z}	0.249	0.247	0.224	0.228	0.122	0.123

b			
Value	$(1+\alpha)_{k_3}^{k_2}$		
	$(1+0.1)_{0.737}^{0.355}$	$(1+0.5)_{0.863}^{0.681}$	$(1+0.9)_{0.973}^{1.352}$
d_0	0.3410	2.1988	1.4352
d_1	4.1726	1.0918	1.2768
d_2	2.9332	0.4552	0.6968
e_0	1.0000	1.0000	1.0000
e_1	3.4545	2.0000	1.1579
e_2	0.7403	0.2000	0.0200

$k_{2,3}$ shown are for minimum passband error

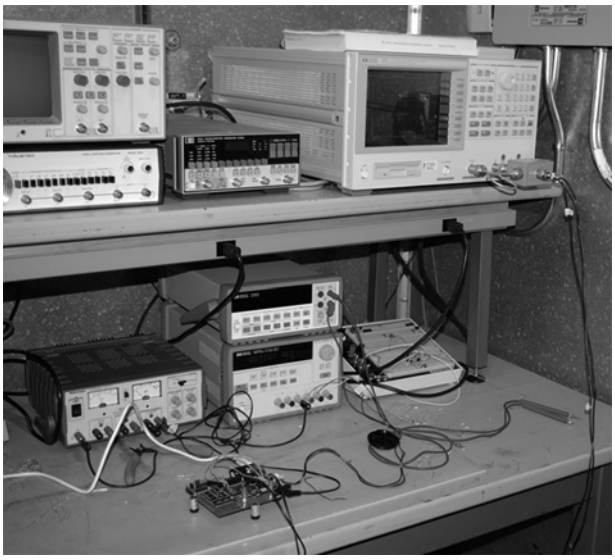

Figure 5 *Test setup to measure the magnitude response of circuits implemented on the AN231E04 with a HP4395A network analyser*

FHPFs are also possible by dividing by the Butterworth polynomial after applying the low-pass to high-pass and frequency shifting transformations. This creates a stable higher-order high-pass fractional filter of order $(n+\alpha)$ that can be written as

$$H^{\mathrm{HP}}_{n+\alpha}(s) = \frac{H^{\mathrm{HP}}_{1+\alpha}(s)}{B^{\mathrm{HP}}_{n-1}(s)}, \quad n \geq 2 \tag{15}$$

where $B^{\mathrm{HP}}_{n}(s)$ is a standard Butterworth polynomial of order n after applying the LP to HP transformation.

5 Simulations and experimental results

To verify the proposed fractional step filters, both low- and high-pass filters of orders $(1+\alpha)$ and $(4+\alpha)$ for $\alpha = 0.1$, 0.5 and 0.9 were designed in the AnadigmDesigner environment using the values from Tables 1*a* and 2*a* and realised on an AN231E04 FPAA development kit from Anadigm. The magnitude responses of the

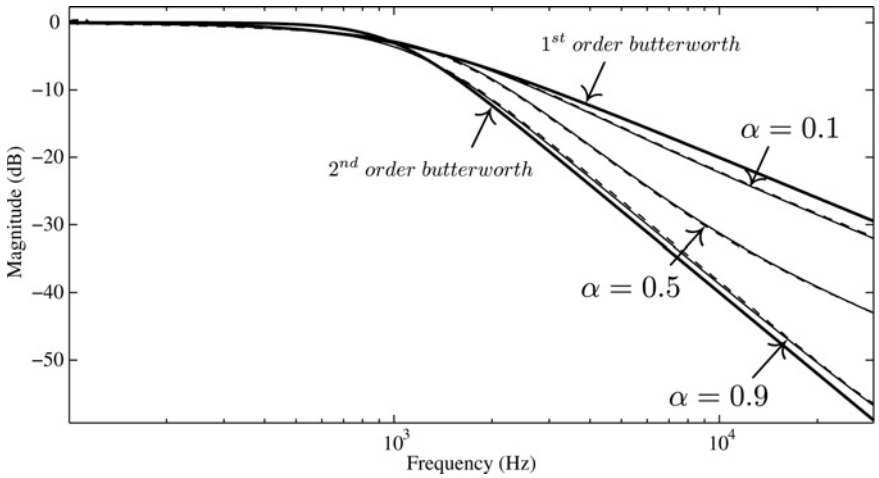

Figure 6 *MATLAB simulation and FPAA experimental results of the magnitude response of the approximated $(1+\alpha)$ order FLPF, shown as solid and dashed lines, respectively, compared against the first- and second-order standard Butterworth low-pass filters*

```
f = linspace(lower_frequency, upper_frequency, num_points); % lower_frequency/upper_frequency in Hz
w = 2*pi*f;
fo = 1e3; wo = 2*pi*fo;
s = 1i*w/wo;
alpha = 0.1;
a0 = (alpha^2+3*alpha+2); a1 = (8-2*alpha^2); a2 = (alpha^2-3*alpha+2);
ApproxSA = (a0*s.^2+a1*s+a2)./(a2*s.^2+a1*s+a0);
k1 = 1; k2 = 0.35; k3 = 0.74;
Hs = k1./(ApproxSA.*(s+k2)+k3);
semilogx(f, 20*log10(abs(Hs)));
```

Algorithm 1 *MATLAB code to simulate and plot FLPF of order $(1+\alpha) = 1.1$ frequency shifted to 1 kHz*

doi: 10.1049/iet-cds.2010.0141

Table 3 Theoretical, simulated and experimental stopband attenuations of approximated $(1+\alpha)$ order FLPF realised using FPAA

Order $(1+\alpha)$	Theoretical, dB/dec	Simulated, dB/dec	Experimental, dB/dec
1.1	−22	−21.34	−21.33
1.5	−30	−30.75	−30.61
1.9	−38	−38.81	−39.00

Table 4 Theoretical, simulated and experimental stopband attenuations of approximated $(4+\alpha)$ order FLPF realised using FPAA

Order $(4+\alpha)$	Theoretical, dB/dec	Simulated, dB/dec	Experimental, dB/dec
4.1	−82	−81.39	−80.80
4.5	−90	−90.76	−90.40
4.9	−98	−98.3	−96.80

implemented fractional step filters were measured using a HP4395A network/spectrum analyser with the test setup being shown in Fig. 5. In the sections that follow, we examine first the approximated fractional step filters followed by an application of the fractional step filter in two tone detection.

5.1 Approximated fractional step filters

In the first of the experimental tests the results of the magnitude response of the approximated first-order FLPFs with fractional steps of 0.1, 0.5 and 0.9 are shown in Fig. 6 as dashed lines, with the corresponding MATLAB simulation results of the theoretical transfer function presented as solid lines. The MATLAB code to simulate and plot the theoretical transfer function of (5) when $\alpha = 0.1$ frequency shifted to 1 kHz is presented in Algorithm 1. The results indicate that the stopband attenuation of the experimental and simulated filters are very close to their theoretical values of $-20(1+\alpha)$ dB/dec. For comparison, these attenuations are listed in Table 3. Note that in both the simulation and experimental results the stopband is not perfectly linear, which is a result of the deviation from the ideal Laplacian operator associated with using the second-order approximation of (3).

In a second test the magnitude response of an approximated fourth-order FLPFs with fractional steps of 0.1, 0.5 and 0.9 was obtained and is shown in Fig. 7 as dashed lines, with the MATLAB simulation results of the theoretical transfer functions presented as solid lines. The experimental results show close agreement with the simulations confirming that the method of implementing a higher-order FLPF by dividing by a higher-order Butterworth polynomial is valid. Also, this method of implementing a higher-order filter maintains the fractional step through the stopband without the passband peaking. Comparing the results, we find that the passband attenuation of the experimental and simulated filters are very close to their theoretical values of $-20(4+\alpha)$ dB/dec. For comparison, these attenuations are listed in Table 4. In a third and final experimental test the results of the $(1+\alpha)$ and $(4+\alpha)$ FHPFs are also shown in Figs. 8 and 9, respectively. MATLAB results are shown alongside as solid lines, with measured stopband attenuations given in Tables 5 and 6, respectively. As before close agreement in the values can be easily observed.

5.2 Application of a fractional step filter

To highlight the precise filtering achieved by a fractional step filter, two tones are applied to an approximated high-pass

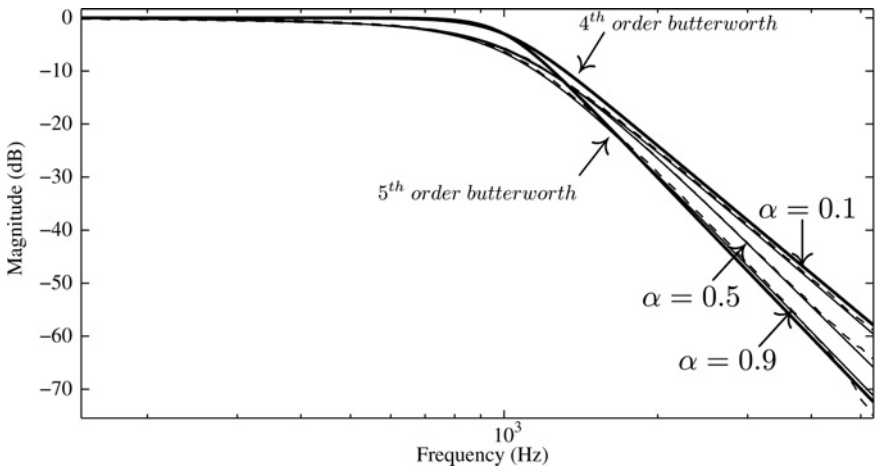

Figure 7 *MATLAB simulation and FPAA experimental results of the magnitude response of the approximated $(4+\alpha)$ order FLPF, shown as solid and dashed lines, respectively, compared against the fourth- and fifth-order standard Butterworth lowpass filters*

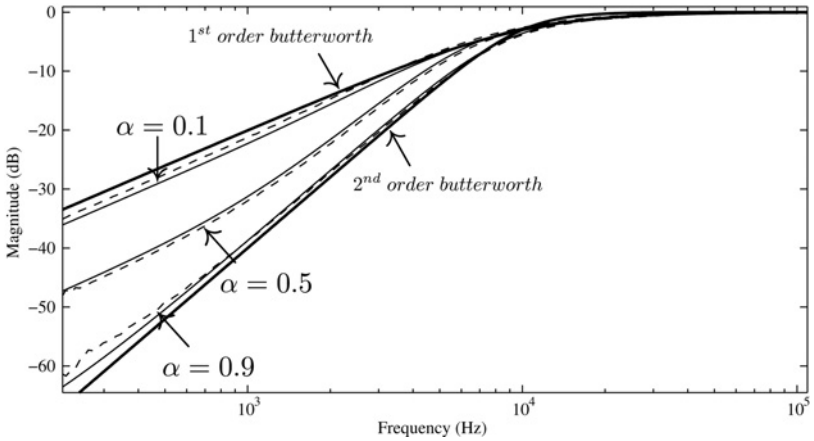

Figure 8 *MATLAB simulation and FPAA experimental results of the magnitude response of the approximated $(1 + \alpha)$ order FHPF, shown as solid and dashed lines, respectively, compared against the first- and second-order standard Butterworth high-pass filters*

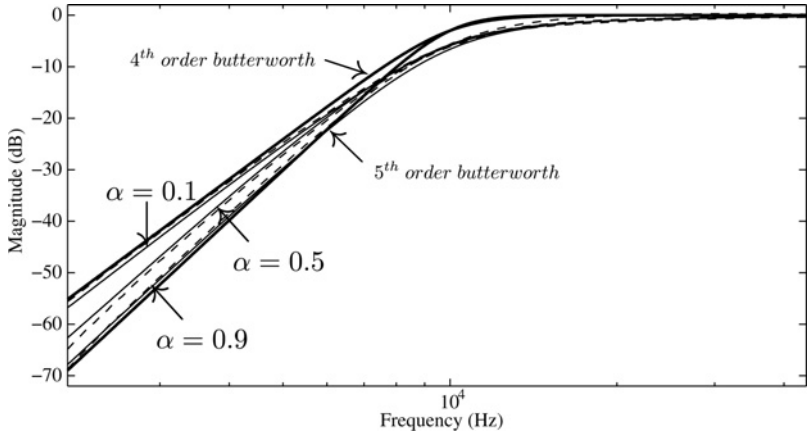

Figure 9 *MATLAB simulation and FPAA experimental results of the magnitude response of the approximated $(4 + \alpha)$ order FHPF, shown as solid and dashed lines, respectively, compared against the fourth- and fifth-order standard Butterworth high-pass filters*

Table 5 Theoretical, simulated and experimental stopband attenuations of approximated $(1 + \alpha)$ order FHPF realised using FPAA

Order $(1 + \alpha)$	Theoretical, dB/dec	Simulated, dB/dec	Experimental, dB/dec
1.1	−22	−21.43	−21.20
1.5	−30	−29.49	−29.80
1.9	−38	−38.82	−37.58

Table 6 Theoretical, simulated and experimental stopband attenuations of approximated $(4 + \alpha)$ order FHPF realised using FPAA

Order $(4 + \alpha)$	Theoretical, dB/dec	Simulated, dB/dec	Experimental, dB/dec
4.1	−82	−81.43	−80.4
4.5	−90	−89.1	−89.6
4.9	−98	−98.74	−99.2

filter of orders $(4 + \alpha) = 4.1$ to 4.9 in steps of 0.2 with the output of the filter measured by the HP4395A network/spectrum analyser to determine the output signal power. Tones at 3 kHz and 10 kHz with peak-to-peak voltages of 500 mV were applied to the approximated FHPFs shifted to a frequency of $f_0 = 10$ kHz. The peak value of the tones for each filter are presented in Table 7. Note that the use

Table 7 Signal power of tones at 3 and 10 kHz after application to approximated FHPFs of orders $(4 + \alpha) = 4.1$ to 4.9 in steps of 0.2

Order $(n + \alpha)$	Power @ 3 kHz, dBm	Power @ 10 kHz, dBm
4.1	−32.7	3.94
4.3	−35.9	3.37
4.5	−38.2	3.5
4.7	−38.4	5.01
4.9	−40.7	4.45

doi: 10.1049/iet-cds.2010.0141

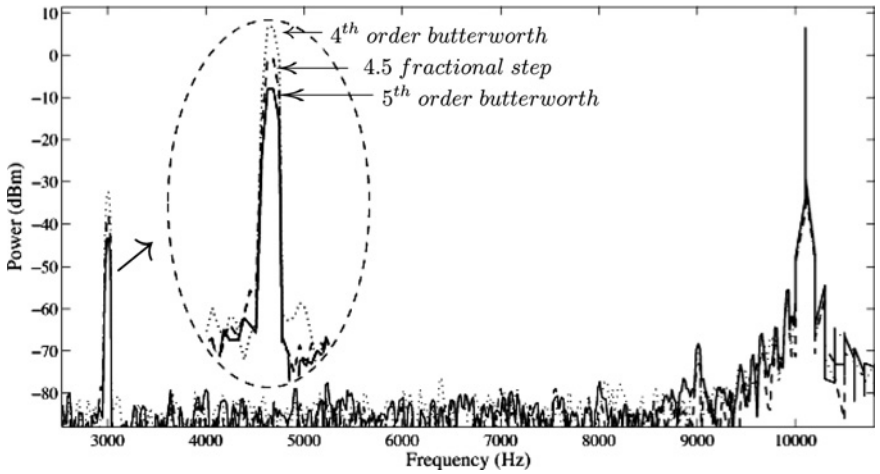

Figure 10 *Frequency spectrum of the approximated 4.5 order FHPF (dashed) compared to fourth (dotted) and fifth (solid) order high-pass Butterworth filters*

of the approximated fractional Laplacian operator results in the deviation of the linear spacing between the powers of the tone at 3 kHz as α increases. This control of the attenuation is not possible using integer order filters. High-pass Butterworth filters, frequency shifted to $f_0 = 10$ kHz, would result in signals of -32.5 and -43.4 dBm for a 3 kHz tone using fourth- and fifth-order filters, respectively. This precise control is also shown in the frequency spectrum of Fig. 10. The spectrum of the fourth- and fifth-order highpass Butterworth filters, as dotted and solid lines, respectively, are compared to that of a 4.5 order FHPF, shown as a dashed line. All of the filters maintain the tone at 10 kHz with the attenuation of the 4.5 order filter at 3 kHz clearly between those of the standard Butterworth filters. These results reinforce the experimental results of the magnitude response in Fig. 9 showing that these filters can be used to precisely control attenuation characteristics.

6 Conclusion

In this paper, we have presented and demonstrated a valid method of fractional filter design using the approximation of (3) and (4)–(5) in extending the design of filters with a flat passband from the integer order to the more general fractional order domain. The implementation of these filters using an FPAA verified this design theory. We have also simulated and physically realised integer order filters that demonstrate a fractional step through the stopband for both high-pass and low-pass filters of orders $(1 + \alpha)$ and $(4 + \alpha)$, all of which show very close agreement between the simulated and experimental results. These results further serve to verify that the low-pass to high-pass transformation does yield a high-pass fractional step filter without peaking in the passband, and that the selection of $k_{2,3}$ for minimum passband error also applies to the FHPFs. Finally, that the method for implementing higher-order fractional step filters is suitable for both low- and high-pass filters. The precise attenuation control of these filters was highlighted in a simple two tone test.

7 References

[1] ORTIGUEIRA M.: 'An introduction to the fractional continuous-time linear systems: the 21st century systems', *IEEE Circuits Syst. Mag.*, 2008, **8**, (3), pp. 19–26

[2] OLDHAM K., SPANIER J.: 'The fractional calculus: theory and applications of differentiation and integration to arbitrary order' (Academic Press, New York, 1974)

[3] PODLUBNY I., PETRAS I., VINAGRE B., O'LEARY P., DORCAK L.: 'Analogue realizations of fractional-order controllers', *Nonlinear Dyn.*, 2002, **29**, pp. 281–296

[4] HABA T., LOUM G., ZOUEU J., ABLART G.: 'Use of a component with fractional impedance in the realization of an analogical regulator of order 1/2', *J. Appl. Sci.*, 2008, **8**, pp. 59–67

[5] MACHADO J., JESUS I., GALHANO A., CUNHA J.: 'Fractional order electromagnetics', *Signal Process.*, 2006, **86**, pp. 2637–2644

[6] MIGUEL F., LIMA M., MACHADO J., CRISOSTOMO M.: 'Experimental signal analysis of robot impacts in a fractional calculus perspective', *J. Adv. Comput. Intell. Intell. Inf.*, 2007, **11**, p. 1079

[7] FERREIRA N.F., DUARTE F., LIMA M., MARCOS M., MACHADO J.T.: 'Application of fractional calculus in the dynamical analysis and control of mechanical manipulators', *Fractional Calc. Appl. Anal.*, 2008, **11**, (1), pp. 91–113

[8] CALDERON A., VINAGRE B., FELIU V.: 'Fractional order control strategies for power electronic buck converters', *Signal Process.*, 2006, **86**, pp. 2803–2819

[9] VARSHNEY P., GUPTA M., VISWESWARAN G.: 'New switched capacitor fractional order integrator', *J. Act. Passive Electron. Devices*, 2007, **2**, pp. 187–197

[10] SANTAMARIA G., VALVERDE J., PEREZ-ALOE R., VINAGRE B.: 'Microelectronic implementations of fractional-order integrodifferential operators', *J. Comput. Nonlinear Dyn.*, 2008, **3**, p. 021301 (6 pp.)

[11] BISWAS K., SEN S., DUTTA P.K.: 'Realization of a constant phase element and its performance study in a differentiator circuit', *IEEE Trans. Circuits Syst. II, Express Briefs*, 2006, **53**, (9), pp. 802–806

[12] AHMAD W., EI-KHAZALI R., ELWAKIL A.: 'Fractional-order wien-bridge oscillator', *Electron. Lett. (UK)*, 2001, **37**, pp. 1110–1112

[13] MAUNDY B., ELWAKIL A., GIFT S.: 'On a multivibrator that employs a fractional capacitor', *Analog Integr. Circuits Signal Process.*, 2010, **62**, (1), pp. 99–103

[14] RADWAN A., SOLIMAN A., ELWAKIL A.: 'First-order filters generalized to the fractional domain', *J. Circuits Syst. Comput.*, 2008, **17**, (1), pp. 55–66

[15] RADWAN A., ELWAKIL A., SOLIMAN A.: 'On the generalization of second-order filters to the fractional-order domain', *J. Circuits Syst. Comput.*, 2009, **18**, (2), pp. 361–386

[16] LAHIRI A., RAWAT T.K.: 'Noise analysis of single stage fractional-order low pass filter using stochastic and fractional calculus', *ECTI Trans. Electr. Eng. Electron. Commun.*, 2009, **7**, (2), pp. 136–143

[17] MATOS C., ORTIGUEIRA M.D.: 'Emerging trends in technological innovation' in CAMARINHA-MATOS L.M., PEREIRA P., RIBEIRO L. (EDS.): 'Fractional filters: an optimization approach' (Springer, 2010), pp. 361–366

[18] FREEBORN T., MAUNDY B., ELWAKIL A.: 'Towards the realization of fractional step filters'. IEEE Int. Symp. on Circuits and Systems (ISCAS), May 2010, pp. 1037–1040

[19] SCHAUMANN R., VALKENBURG M.E.V.: 'Design of analog filters' (Oxford University Press, New York, 2001)

[20] DELIYANNIS T., SUN Y., FIDLER J.: 'Continuous time active filter design' (CRC Press LLC, New York, 1999)

[21] ZVEREV A.I.: 'Handbook of filter synthesis' (John Wiley and Sons, New York, 1967)

[22] WESTERLUND S.: 'Dead matter has memory! [capacitor model]', *Phys. Scr. (Sweden)*, 1991, **43**, pp. 174–179

[23] WESTERLUND S., EKSTAM L.: 'Capacitor theory', *IEEE Trans. Dielectr. Electr. Insul.*, 1994, **1**, (5), pp. 826–839

[24] KRISHNA B., REDDY K.: 'Active and passive realization of fractance device of order 1/2', *Act. Passive Electron. Compon.*, 2008, **2008**, p. 5

[25] DJOUAMBI A., CHAREF A., BESANCON A.: 'Optimal approximation, simulation and analog realization of the fundamental fractional order transfer function', *Int. J. Appl. Math. Comput. Sci.*, 2007, **17**, (4), pp. 455–462

[26] Anadigm: '3rd Generation dynamically reconfigurable dpASP'. AN231E04 Datasheet Rev 1.1, 2007

[27] HUELSMAN L.P.: 'Active and passive analog filter design: an introduction' (McGraw-Hill, Inc., 1993)

[28] FRIEND J., HARRIS C., HILBERMAN D.: 'Star: an active biquadratic filter section', *IEEE Trans. Circuits Syst.*, 1975, **CAS-22**, pp. 115–121

doi: 10.1049/iet-cds.2010.0141